Biophysical Journal, Volume 98

Supporting Material

LCP-Tm: an Assay to Measure and Understand Stability of Membrane Proteins in a Membrane Environment

Wei Liu, Michael A. Hanson, Raymond C. Stevens, and Vadim Cherezov

SUPPORTING MATERIAL

LCP-Tm: an assay to measure and understand stability of membrane proteins in a membrane environment.

Wei Liu, Michael A. Hanson, Raymond C. Stevens, and Vadim Cherezov

SUPPLEMENTAL MATERIALS AND METHODS

Expression and Purification of β_2AR constructs. Two engineered human β_2-adrenergic receptor constructs were used in this study. The first construct, β_2AR, contained a stabilizing mutation E122W (1), C-terminal truncation at residue 348, mutated out glycosylation site N187E (2,3), and deletion of residues 245 to 259 in the third intracellular loop (ICL3). In addition to all initial modifications, the second construct, β_2AR-T4L, included a replacement of the ICL3 residues 231 to 262 between transmembrane helices 5 and 6 with cysteine-free T4 lysozyme (C54T, C97A) residues 2 to 161 (3). Both constructs had a FLAG tag at the N-terminus and a 6xHis tag at the C-terminus. These two constructs were incorporated into the baculovirus AcMNPV genome using site specific recombination in *E. coli* followed by transfection and viral passaging in insect cells to generate high-titer viral stocks (Bac-to-Bac system, Invitrogen, Carlsbad, CA). Viral stocks were used to infect *Spodoptera frugiperda* (Sf9) insect cells for protein expression as described previously (2). The cells were lysed by a douncer and the membrane fraction was isolated, extensively washed and treated with iodoacetamide (Sigma, St. Louis, MO). After solubilization of isolated membranes with 0.5% w/v n-Dodecyl-β-D-maltopyranoside (DDM, Anatrace, Maumee, OH) and 0.1% w/v cholesteryl hemisuccinate (CHS) the protein was purified in the presence of 500 μM timolol (Sigma) using a cobalt-charged TALON Superflow IMAC (Clontech, Mountain View, CA) and a nickel-charged Sepharose 6 Fast Flow IMAC (GE Healthcare, Piscataway, NJ) gravity columns sequentially. The protein was de-glycosylated by incubating with PNGaseF (NEB, Ipswich, MA) at 4°C overnight on the nickel-charged IMAC column. PNGaseF was washed off using 5 column volumes (CV) of 20 mM Hepes pH 7.5, 150 mM NaCl, 0.05% w/v DDM, 0.01% w/v CHS, and 500 μM timolol. The purity and monodispersity were examined by SDS-PAGE and analytical size exclusion chromatography (SEC) using a SepaxNanofilm SEC-250 column (Sepax, Newark, DE) on a Dionex (Sunnyvale, CA) Ultimate HPLC system. The mobile phase for SEC was 20 mM Hepes pH 7.5, 150 mM NaCl, 2% v/v glycerol, 0.05% w/v DDM, 0.01% w/v CHS. Protein used in subsequent experiments was more than 95% pure by SDS-PAGE and run as a single peak on SEC. For the ligands effect studies, the receptor was purified in a timolol bound state. The ligand was exchanged for 100 μM carazolol (TRC, North York, On., Canada), 500 μM timolol, alprenolol (Sigma) or clenbuterol (Sigma), respectively, using 10 CV wash on the nickel-charged IMAC column. An apo-protein was obtained by washing the resin with 100 CV of the ligand-free buffer. The protein was eluted in a minimal volume of the same buffer used for the ligand exchange, supplemented with 200 mM imidazole, with the exception that no ligand was used in the elution buffer for the carazolol-bound receptor in order to reduce concentration of free carazolol in solution. Protein concentration was determined by integration of the 280 nm absorption peak on the SEC elution profile and comparing it with a calibration curve obtained for a BSA standard (Sigma). Timolol-bound protein was stored at 4°C and used within 3 weeks, during which no change in the aggregation state of the protein and the melting temperature, Tm, were detected. Protein bound to other ligands as well as the apo-protein were used immediately upon ligand exchange/wash procedure.

SUPPLEMENTAL RESULTS

Optimization of the LCP-Tm protocol.

Due to the issue of LCP clouding upon heating, we designed a novel approach to assess the thermal stability of membrane proteins in LCP. This approach contains rather unconvential treatments: instead of a temperature ramping, the LCP-Tm protocol required heating and cooling steps with at least two different incubation periods per each data point, one at an elevated temperature and one at 20°C during centrifugation in order to achieve LCP transparency. The assumption was that the denaturing effect of the temperature on the intrinsic protein fluorescence remains fixed upon cooling, so that it could be accurately measured at room temperature, and that this effect is accumulating with the subsequent temperature treatment steps until all protein is denatured. To verify this assumption and to optimize the incubation times we performed the following experiments.

First, we prepared several samples of β_2AR-T4L/timolol in the monoolein (MO)-based LCP, heated them to the mid-transition temperature of 45°C and incubated for different periods of time ranging from 2 to 45 min, then cooled them down, centrifuged and analyzed at room temperature (RT, 21-23°C). The fluorescence signal increased upon incubation as expected until it reached a plateau at ~1.36 for the samples incubated for 5-7 min and stayed at this value for up to at least 30 min incubation (Fig. S5 *A*). A slight increase in the signal of about 3 standard deviations was observed for the samples incubated for 45 min. A slow increase in fluorescence upon prolonged incubation at elevated temperatures would be expected since these highly unstable proteins slowly denature with time even at RT (see Fig. 5). The positive outcome of this experiment is that the signal achieves a plateau in the 5-30 min range, which has the same value as the signal obtained after reaching 45°C in the LCP-Tm assay (see Fig. 3). Based on these results the incubation time at each temperature was fixed to 7 min to ensure full equilibration and to minimize the time for acquiring each data point, however, an equally accurate data can be obtained with 5-30 min incubation times.

The second set of experiments was designed to check whether the increase in the intrinsic fluorescence achieved after a heating would stay constant or reverse back to the original value upon incubation at RT. One set of β_2AR-T4L/timolol in the MO-based LCP samples was heated to the mid-transition temperature of 45°C, while another set was heated to the end transition temperature of 80°C. Samples were incubated for 10 min at their corresponding temperatures, cooled down, centrifuged and analyzed at RT at regular time intervals for a total incubation of 8 h (Fig. S5 *B*). The intrinsic fluorescence of both sets of samples increased to the same values as those obtained after reaching the corresponding temperatures using the LCP-Tm protocol, confirming that the recorded fluorescence signals depend only on the final incubation temperature and not on the number of heating/cooling steps used before reaching it. The fluorescence signal did not decrease upon 8 h of incubation in either of the samples, indicating that the changes in the protein induced by the temperature treatment were irreversible. A slow increase in the fluorescence amounting to about 3 standard deviations after 4 h of incubation was observed for the samples treated at 45°C. Such a slow increase was expected as previously noted. No change in the fluorescence signal of the samples treated at 80°C was observed, suggesting that the protein was fully denatured by this temperature treatment. Based on the results of these experiments we decided to analyze the samples immediately after achieving transparency of LCP (10-15 min of centrifugation at 20°C). Longer centrifugation times or incubations at RT for up to 3 h should not have any significant impact on the data obtained.

The data discussed in this section confirm that the LCP-Tm protocol provides a robust way for measuring changes in the intrinsic protein fluorescence upon heating. The measured fluorescence signal does not depend on the number of steps. We have used 5°C increments between incubation temperatures as an optimum compromise between the adequate sampling interval and the time required to collect a

complete denaturation curve. Curve fitting of the data collected in this study provided highly accurate values for the transition temperature (see section on Accuracy and Reproducibility). Sharper transitions, however, may require smaller increments between incubation temperatures for capturing them accurately.

Accuracy and reproducibility.

To assess the reproducibility of the LCP-Tm protocol, we applied it to 15 independently prepared samples of β_2AR-T4L/timolol in the MO-based LCP using protein from 5 independently purified batches. The results are shown in Table S2 and the averaged data are plotted in Fig. 3 *A*. Fitting data for each sample separately with the Boltzmann sigmoidal curve gave values of melting temperatures, Tm, with small fitting errors of 0.2 – 0.5°C. Reproducibility of the Tm data was very high as evidenced by low data scattering from 15 independent samples with the lowest Tm = 45.8°C and the highest Tm = 46.7°C. Averaging all data resulted in Tm = 46.4 ± 0.3°C. Such a remarkable accuracy and reproducibility of the LCP-Tm assay provided high sensitivity for comparing the thermal stability of different proteins and protein constructs in LCP as well as the effects of ligands, host lipids and additives. For all subsequent experiments conducted in this study we report the averaged data collected on at least three samples with the error representing the standard deviation of these measurements.

On the origin of the fluorescence increase.

Our observations of the increase in the intrinsic fluorescence upon thermal denaturation of membrane proteins in LCP (Fig. 3 *A*) contradict a common knowledge derived from unfolding studies of soluble proteins, in which exposure of tryptophan residues to a polar solvent environment induces a decrease in the fluorescence yield along with a red shift of the emission maximum (4). To understand the origin of the apparent ~75% increase in the fluorescence upon thermal denaturation of β_2AR-T4L/timolol in LCP, we conducted two experiments. First, ligand depletion experiments performed at RT resulted in the same 75% increase in fluorescence as in the thermal denaturation experiments (compare Figs. S2 and S6). Addition of ligand to the depleted samples restored the intrinsic fluorescence to the original level (Fig. S6), indicating that the apo-receptor remained functional in LCP. Second, thermal denaturation of the apo- protein in LCP did not affect its intrinsic fluorescence, but did render the protein non-functional, abolishing its ability to bind ligands. Based on these data, we concluded that the entire observed increase in intrinsic protein fluorescence in the LCP-Tm assay can be attributed to an irreversible ligand release caused by protein unfolding. Similar effects of the ligand binding/dissociation on the intrinsic protein fluorescence have been previously described and used to measure the ligand binding affinities (5-7).

It is important to note that upon passing through the cubic-Pn3m/inverse hexagonal H_{II} phase transition at ~90°C (see Fig. 2 *B*) the intrinsic fluorescence of β_2AR-T4L sharply decreased by ~30% (Fig. S7). The drop in fluorescence was accompanied by a red shift in the emission peak (Fig. S7 *B*) suggesting that at least some tryptophan residues changed their environment into a more polar one. Similar drop in fluorescence at 90°C was observed regardless of the ligand used as well as for the apo-receptor (data not shown). We reconciled these observations with a view that as long as the LCP remains intact (17–90°C for the MO-based LCP), the temperature-induced increase in the intrinsic protein fluorescence is solely due to the irreversible ligand release. Transition to the H_{II} phase, however, disrupts the lipid bilayer, exposing at least some tryptophan residues to a polar environment and inducing a decrease in the intrinsic fluorescence along with a red shift. Therefore, in order to obtain meaningful results with the LCP-Tm assay, the sample should remain in LCP during the entire course of measurements. This was the reason why 80°C was chosen as the end point in the LCP-Tm protocol. Some additives can decrease the cubic-Pn3m/H_{II} phase transition temperature to a degree where it would

interfere with the protein denaturation temperature. Such conditions can be easily identified by a sharp drop and a red shift in the intrinsic fluorescence and should be avoided. All samples used in this study remained in LCP unless noted otherwise.

Supplemental references.

1. Roth, C. B., M. A. Hanson, and R. C. Stevens. 2008. Stabilization of the human beta2-adrenergic receptor TM4-TM3-TM5 helix interface by mutagenesis of Glu122(3.41), a critical residue in GPCR structure. *J. Mol. Biol.* 376:1305-1319.
2. Hanson, M. A., V. Cherezov, M. T. Griffith, C. B. Roth, V. P. Jaakola, et al. 2008. A specific cholesterol binding site is established by the 2.8 A structure of the human beta2-adrenergic receptor. *Structure.* 16:897-905.
3. Rosenbaum, D. M., V. Cherezov, M. A. Hanson, S. G. Rasmussen, F. S. Thian, et al. 2007. GPCR engineering yields high-resolution structural insights into beta2-adrenergic receptor function. *Science.* 318:1266-1273.
4. Lakowicz, J. R. 1983. Instrumentation of fluorescence spectroscopy, Plenum Press, New York, NY.
5. Cherezov, V., E. Yamashita, W. Liu, M. Zhalnina, W. A. Cramer et al. 2006. *In meso* structure of the cobalamin transporter, BtuB, at 1.95 A resolution. *J. Mol. Biol.* 364:716-734.
6. Cherezov, V., W. Liu, J. P. Derrick, B. Luan, A. Aksimentiev et al. 2008. *In meso* crystal structure and docking simulations suggest an alternative proteoglycan binding site in the OpcA outer membrane adhesion. *Proteins.* 71:24-34.
7. Ruan, K.-H., V. Cervantes, and J. Wu. 2009. Ligand-specific conformation determines agonist activation and antagonist blockade in purified human thromboxane A2 receptor. *Biochemistry.* 48:3157-3165.
8. Briggs, J, and M. Caffrey. 1994. The temperature-composition phase diagram of monomyristolein in water: equilibrium and metastability aspects. *Biophys. J.* 66:573-587.
9. Manalan, A. S., H. R. Besch, Jr., and A. M. Watanabe. 1981. Characterization of [^{3}H](±)carazolol binding to β-adrenergic receptors. *Circ. Res.* 49:326-336
10. Baker, J. G. 2005. The selectivity of β-adrenoceptor antagonists at the human β1, β2 and β3 adrenoceptors. *British J. Pharmacol*. 144:317-322.
11. Hoffmann, C., M. R. Leitz, S. Oberdorf-Maass, M. J. Lohse, and K.-N. Klotz. 2004. Comparative pharmacology of human β-adrenergic receptor subtypes – characterization of stably transfected receptors in CHO cells. *Naunyn-Schmiedeberg's Arch. Pharmacol.* 369:151-159.
12. Del Carmine, R., C. Ambrosio, M. Sbraccia, S. Cotecchia, A. P. Ijzerman et al. 2002. Mutations inducing divergent shifts of constitutive activity reveal different modes of binding among catecholeamine analogues to the b2-adrenergic receptor. *British J. Pharmacol.* 135:1715-1722.
13. Liu, W., and M. Caffrey. 2005. Gramicidin structure and disposition in highly curved membranes. *J. Struct. Biol.* 150:23-40.
14. Qiu, H., and M. Caffrey. 1998. Lyotropic and thermotropic phase behavior of hydrated monoacylglycerols: Structure characterization of monovaccenin. *J. Phys. Chem. B.* 102:4819–4829.

15. Clogston, J., and M. Caffrey. 2005. Controlling release from the lipidic cubic phase. Amino acids, peptides, proteins and nucleic acids. *J. Contr. Release.* 107:97-111.

16. Alexandrov, A. I., M. Mileni, E. Y. Chien, M. A. Hanson, and R. C. Stevens. 2008. Microscale fluorescent thermal stability assay for membrane proteins. *Structure.* 16:351-359.

Table S1. Unique* membrane proteins with high resolution structures obtained by *in meso* crystallization.

	Protein name	Source organism	LCP lipid	Mesophase	Number of structures	Best resolution, Å
1	bacteriorhodopsin	*Halobacterium salinarum*	monoolein	cubic	33	1.43
2	halorhodopsin	*Halobacterium salinarum*	monoolein	cubic	3	1.70
3	sensory rhodopsin II	*Natronomonas pharaonis*	monoolein	cubic	4	2.10
4	sensory rhodopsin II / transducer	*Natronomonas pharaonis*	monovaccenin	cubic	3	1.93
5	sensory rhodopsin	*Nostoc sp. pcc 7120*	monoolein	cubic	1	2.00
6	reaction center	*Rhodobacter sphaeroides*	monoolein	sponge	4	2.20
7	reaction center	*Blastochloris viridis*	monoolein	sponge	2	1.86
8	light harvesting complex 2	*Rhodoblastus acidophilus*	monoolein	sponge	1	2.45
9	outer membrane vitamin B_{12} transporter BtuB	*E. coli*	monoolein	sponge	1	1.95
10	outer membrane adhesin OpcA	*Neisseria meningitidis*	monoolein	cubic	1	1.95
11	β2-adrenergic receptor	*Homo sapiens*	monoolein / cholesterol	cubic / sponge	2	2.4
12	adenosine A_{2A} receptor	*Homo sapiens*	monoolein / cholesterol	cubic	1	2.6

* By unique proteins we consider those that have less than 80% of sequence identity. Therefore, proteins with the same name but from different sources, such as reaction center from *R. sphaeroides* and *B. viridis*, are typically considered as different. Additionally, the complex between sensory rhodopsin II and transducer is considered to be different from sensory rhodopsin II due to a significant (more than 20%) contribution of the transducer into the total size of the complex. Multiple mutants and intermediate photocycle states of bacteriorhodopsin as well as different ligand-bound states of β2-adrenergic receptor are not considered to be unique.

Table S2. Accuracy and reproducibility of the LCP-Tm assay. LCP-Tm results for 15 independently prepared samples of β_2AR-T4L/timolol in the MO-based LCP using protein from 5 independently purified batches. For each individual sample the fitting results along with the errors reported by GraphPad Prizm software are shown. The averaged values represent mean +/- SD (standard deviation) of data from 15 samples.

β_2AR-T4L/ timolol	**Slope, °C**	**Tm, °C**
Sample 1	3.3 ± 0.3	46.4 ± 0.3
Sample 2	3.1 ± 0.2	46.0 ± 0.2
Sample 3	3.1 ± 0.4	45.8 ± 0.4
Sample 4	3.3 ± 0.2	46.6 ± 0.3
Sample 5	3.5 ± 0.4	46.7 ± 0.4
Sample 6	2.9 ± 0.4	46.3 ± 0.2
Sample 7	3.1 ± 0.2	45.9 ± 0.5
Sample 8	3.8 ± 0.4	46.4 ± 0.3
Sample 9	2.9 ± 0.5	46.5 ± 0.2
Sample 10	3.4 ± 0.3	46.7 ± 0.5
Sample 11	3.3 ± 0.4	46.1 ± 0.3
Sample 12	3.5 ± 0.4	46.7 ± 0.3
Sample 13	3.2 ± 0.3	46.6 ± 0.2
Sample 14	3.6 ± 0.5	46.0 ± 0.4
Sample 15	3.1 ± 0.4	46.5 ± 0.4
Average	3.3 ± 0.3	46.4 ± 0.3

Table S3. Summary of the LCP-Tm assay data. Reported values and errors represent the averaged fitting results and their standard deviations obtained from at least 3 samples.

β_2AR-T4L	Hydration*, %w/w	Slope, °C	Tm, °C	Increase in F, %
Ligands				
Apo- (CPM)	40	4.3 ± 0.3	37.2 ± 0.4	329 ± 18
Clenbuterol	40	4.0 ± 0.3	43.0 ± 0.2	76.5 ± 5.0
Alprenolol	40	4.6 ± 0.2	44.5 ± 0.2	68.8 ± 3.5
Timolol	40	3.3 ± 0.3	46.4 ± 0.3	77.5 ± 5.0
Timolol (CPM)	40	5.1 ± 0.6	47.3 ± 0.7	333 ± 12
Carazolol	40	3.5 ± 0.2	50.8 ± 0.2	74.8 ± 3.3
Carazolol (CPM)	40	4.8 ± 0.5	51.5 ± 0.5	316 ± 7
LCP host lipid				
Monoolein	40	3.3 ± 0.3	46.4 ± 0.3	77.5 ± 5.0
Monopalmitolein	50	4.7 ± 0.3	43.5 ± 0.4	80.0 ± 3.2
Monovaccenin	50	3.5 ± 0.3	39.1 ± 0.2	77.0 ± 2.5
Monoeicosenoin	40	3.3 ± 0.4	35.0 ± 0.3	83.9 ± 5.7
Lipid additives				
No additives	40	3.3 ± 0.3	46.4 ± 0.3	77.5 ± 5.0
Cholesterol	40	3.7 ± 0.4	48.7 ± 0.3	76.9 ± 2.8
DOPC	40	4.4 ± 0.4	40.8 ± 0.5	80.7 ± 3.3
DOPE	40	3.2 ± 0.3	43.8 ± 0.3	74.2 ± 2.4
DOPS	40	3.7 ± 0.3	43.1 ± 0.2	76.1 ± 4.4
DOPG	40	3.5 ± 0.3	44.4 ± 0.3	77.0 ± 4.8
Buffer pH				
8.0	40	4.2 ± 0.2	45.2 ± 0.2	72.8 ± 2.0
7.5	40	3.3 ± 0.3	46.4 ± 0.3	77.5 ± 5.0
6.0	40	4.4 ± 0.2	43.4 ± 0.2	80.4 ± 4.3
4.0	40	4.2 ± 0.3	37.3 ± 0.3	80.1 ± 1.6
Hydration, %wt/wt				
40	40	3.3 ± 0.3	46.4 ± 0.3	77.5 ± 5.0
35	35	3.2 ± 0.2	45.8 ± 0.2	79.6 ± 3.3
30	30	2.2 ± 0.2	39.6 ± 0.3	81.3 ± 2.1
Effect of mesophase				
No treatment	40	3.3 ± 0.3	46.4 ± 0.3	77.5 ± 5.0
Lc	40	3.6 ± 0.2	42.8 ± 0.4	34.6 ± 2.8
H_{II}	40	4.2 ± 0.2	44.4 ± 0.4	46.3 ± 2.5
Lα (low hydration)	40	3.7 ± 0.3	43.5 ± 0.2	60.0 ± 2.0
Lα (detergent)	40	3.7 ± 0.5	45.8 ± 0.2	72.7 ± 1.8

Table S3 continued. Summary of the LCP-Tm assay data. Reported values and errors represent the averaged fitting results and their standard deviations obtained from at least 3 samples.

Bacteriorhodopsin (bR)	**Hydration*, %w/w**	**Slope, °C**	**Tm, °C**	**Increase in F, %**
No additive	40	5.4 ± 0.5	43.8 ± 0.6	400 ± 19
1 M Na/K Phosphate	35	4.6 ± 0.5	50.7 ± 0.4	385 ± 28
Excess retinal	40	5.4 ± 0.4	46.3 ± 0.4	380 ± 10
β_2AR	**Hydration*, %w/w**	**Slope, °C**	**Tm, °C**	**Increase in F, %**
Timolol	40	4.3 ± 0.4	40.5 ± 0.5	69.0 ± 4.6
Carazolol	40	4.2 ± 0.3	44.2 ± 0.4	70.2 ± 6.4
Timolol + Cholesterol	40	3.9 ± 0.3	44.0 ± 0.3	75.4 ± 2.9

* The target hydration values are reported in the table. The actual hydration values for the corresponding samples were within 2 %w/w of the target values, as verified by the "bubble" method (8).

Table S4. Correlations between the ligand binding, stability and crystal quality for β_2AR-T4L.

Ligand	Ki*, nM	Tm†, °C (intrinsic)	Tm†, °C (CPM)	Resolution, Å	Crystal size, μm	Number of trials‡
Carazolol	0.02 (9)	50.8 ± 0.2	51.5 ± 0.5	2.4	40 x 15 x 5	12864 [4512]
Timolol	0.21 (10)	46.4 ± 0.3	47.3 ± 0.7	2.8	30 x 10 x 4	7008 [3168]
Alprenolol	1.2 (11)	44.5 ± 0.2	-	3.5	25 x 6 x 6	3744 [1344]
Clenbuterol	33 (12)	43.0 ± 0.2	-	~7	30 x 8 x 5	6336 [960]
Apo-	-	-	37.2 ± 0.4	-	-	288 [182]

* References to the data on typical ligand dissociation constants obtained from competition binding experiments are shown in parenthesis.

† Unfolding temperatures, Tm, in MO cubic phase were measured in this work by using either intrinsic protein fluorescence or fluorescence from a thiol-binding dye CPM following the LCP-Tm protocol.

‡ Total number of crystal optimization trials and number of unique conditions (in square brackets) are reported. Crystal optimization trials continued until no improvements to the crystal size were detected. For the apo-receptor no crystals were obtained in 288 total trials (182 unique conditions), derived from the combined successful conditions yelding crystals in the previous trials with ligand-bound receptors. All crystallization trials were performed in MO cubic phase supplemented with 10 %w/w cholesterol.

Table S5. Correlations between structural parameters of LCP made of different lipids (at 20°C and full hydration) and β_2AR-T4L/timolol unfolding temperature.

Lipid	Lipid bilayer thickness, Å	Water channel diameter, Å	Tm, °C
Monopalmitolein	33.2 (13)	56.6 (13)	43.5 ± 0.4
Monoolein	35.6 (13)	46.4 (13)	46.4 ± 0.3
Monovaccenin	36.4 (14)	66 (14)	39.1 ± 0.2
Monoeicosenoin	37.4 (13)	45.5 (13)	35.0 ± 0.3

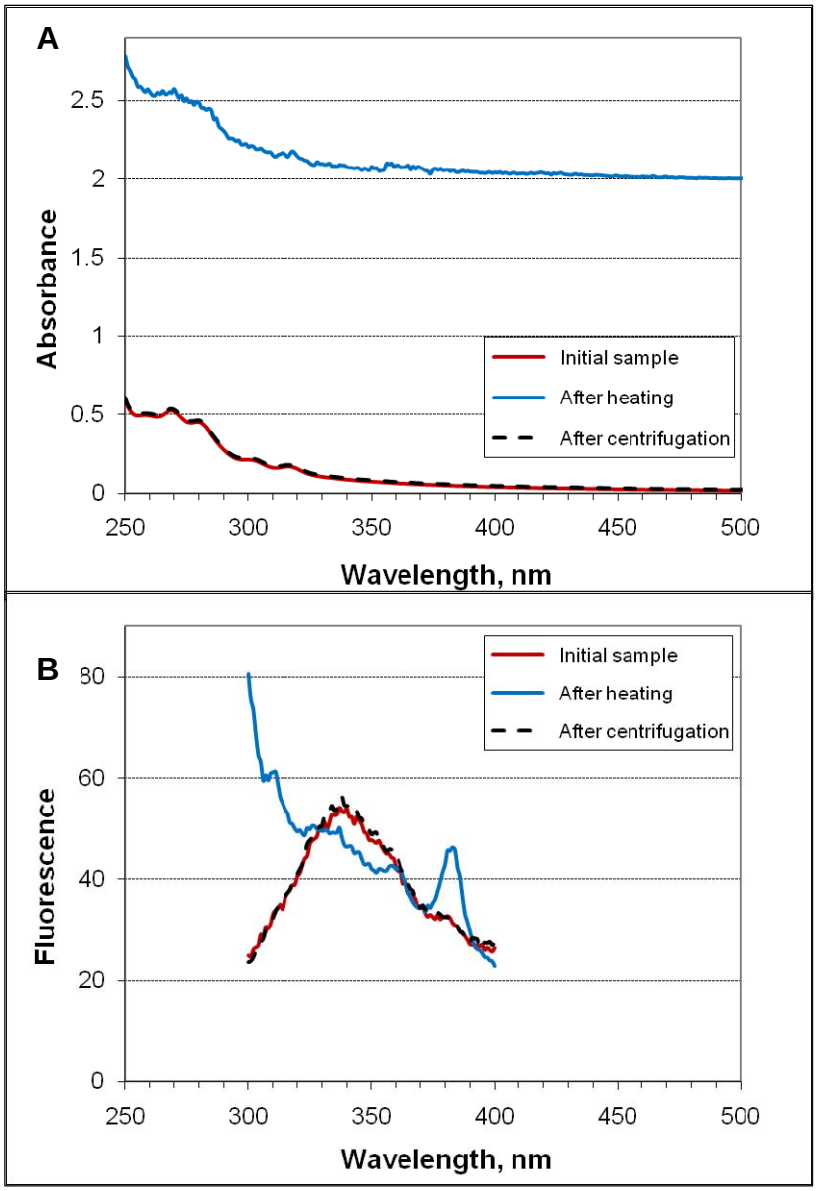

Figure S1. Spectroscopic characteristics of an LCP sample. Absorbance (*A*) and fluorescence (excitation at 280 nm) (*B*) spectra of a background LCP sample (MO mixed with 40% w/w of 20 mM HEPES buffer, pH 7.5). The fluorescence spectra in (*B*) were not corrected for the inner filter effect. The sample was prepared at RT (red trace); heated to 80°C and cooled down to RT (blue trace); finally, centrifuged at 5,600 × g and 20°C for 10 min (black dash trace). Few small absorbance peaks in (*A*) are from extremely low, undetected by thin layer chromatography impurities in MO. These impurities, at different levels, are present in all commercial sources of MO that we have tried. The same lot of MO was used throughout this study for proper background corrections. Fluorescence signal measured from the sample after heating in (*B*), blue trace, is dominated by scattering and, thus, mostly reflects the bulb spectrum leaking from the monochromator. Peak at ~380 nm is one of the bulb's emission lines. This figure demonstrates that LCP after heating is not usable for spectroscopic measurements. Centrifugation returns it back into the original transparent state.

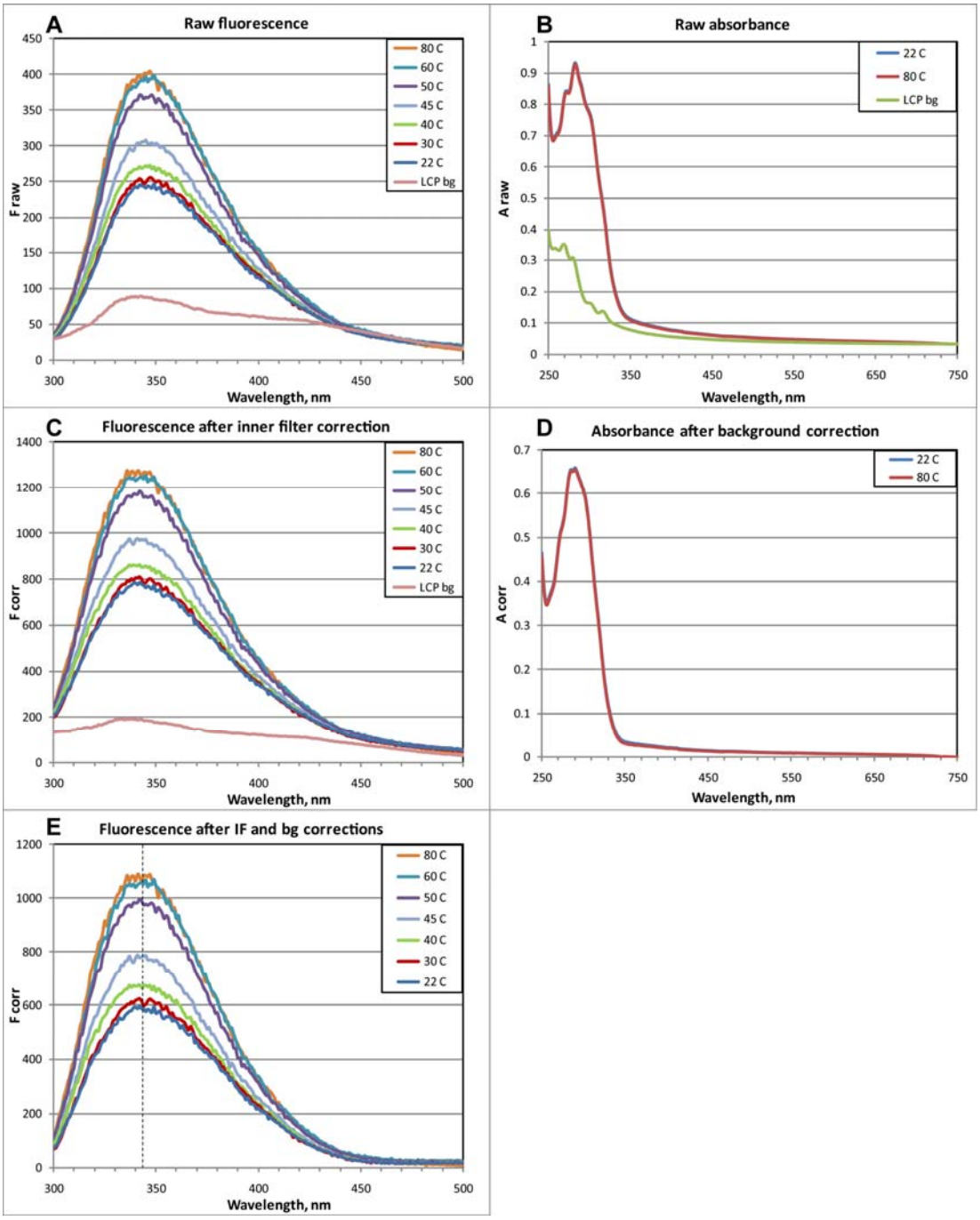

Figure S2. Raw and corrected intrinsic fluorescence (excitation at 280 nm) and absorbance spectra recorded by the LCP-Tm for β_2AR-T4L/timolol in the MO cubic phase. For clarity data are shown for selected temperature treatments only. The protein and background absorbance as well as the background fluorescence did not change upon temperature treatments. The fluorescence emission peak stayed constant at 342 nm in the whole temperature range 22 – 80°C. The maximum fluorescence emission signal at 342 nm (*E*) was used to plot the curve in Fig. 3 *A*. All spectra were collected at RT.

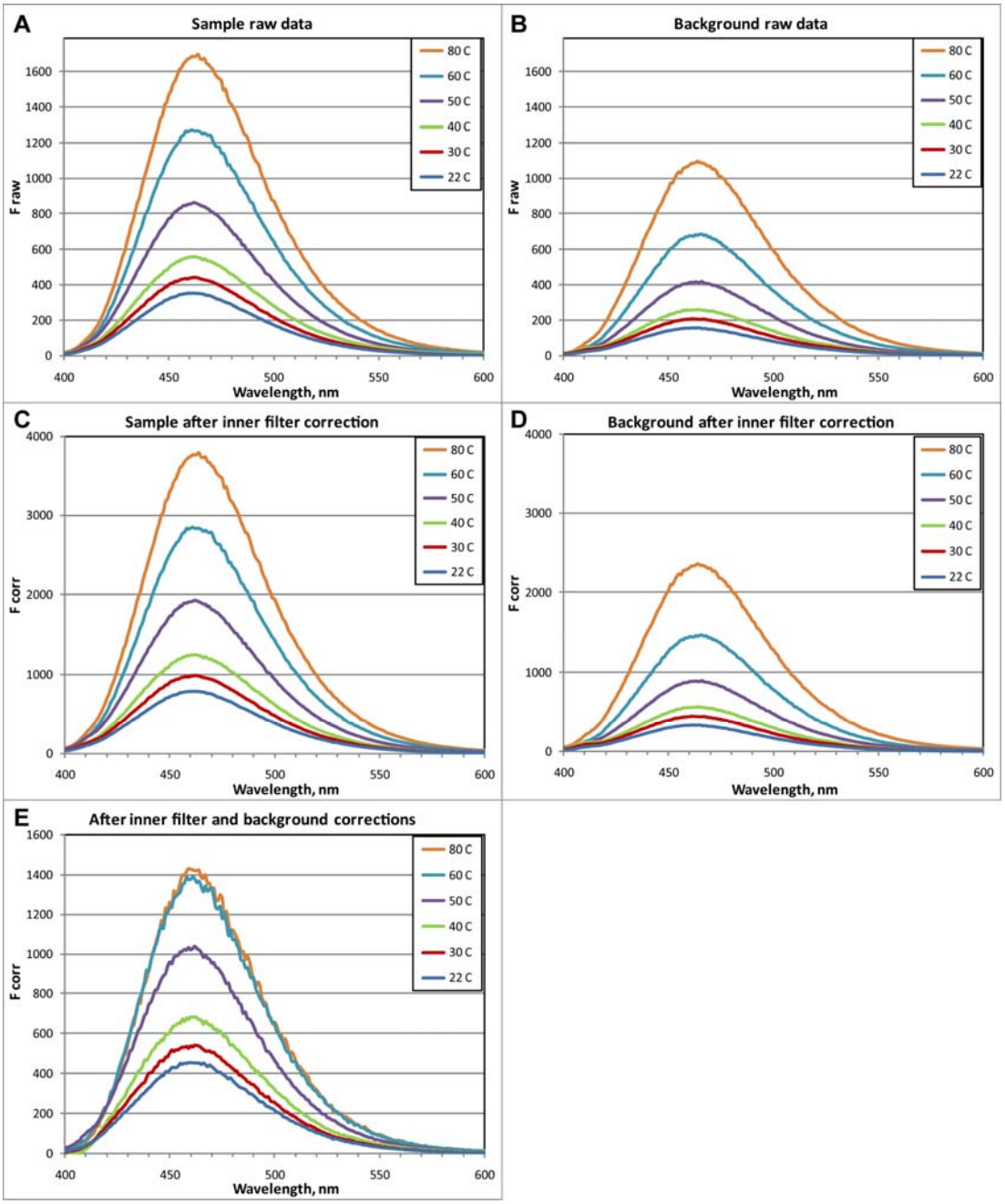

Figure S3. Raw and corrected fluorescence spectra recorded by the LCP-Tm in the presence of CPM for β_2AR-T4L/timolol in the MO cubic phase using excitation at 380 nm. For clarity data are shown for selected temperatures only. Fluorescence from the background sample increased with the temperature treatments (*B, D*). The inner filter corrections were based on the absorbance data shown in Fig. S9. The emission maxima of the corrected spectra remained at 462 nm after all temperature treatments and were used to make Fig. 3 *A*.

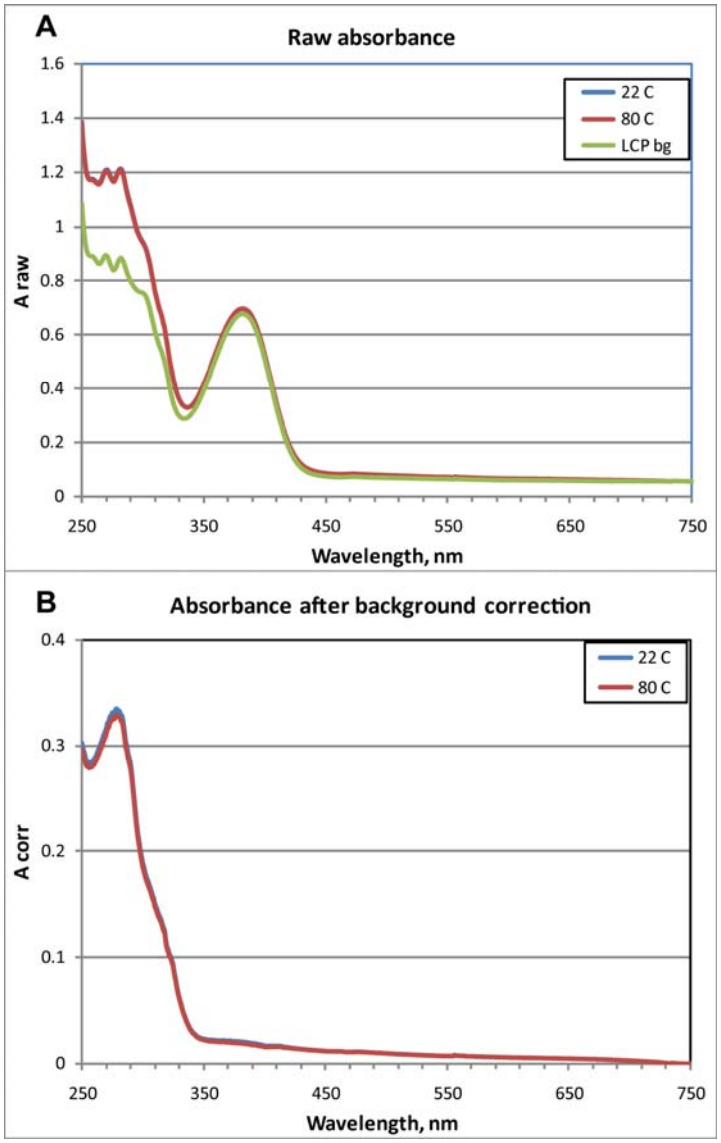

Figure S4. Raw and corrected absorbance spectra recorded by the LCP-Tm in the presence of CPM for β_2AR-T4L/timolol in the MO cubic phase. The absorbance spectra of both protein and background samples did not change with temperature treatments. A peak at ~380 nm (*A*) corresponds to absorbance from CPM.

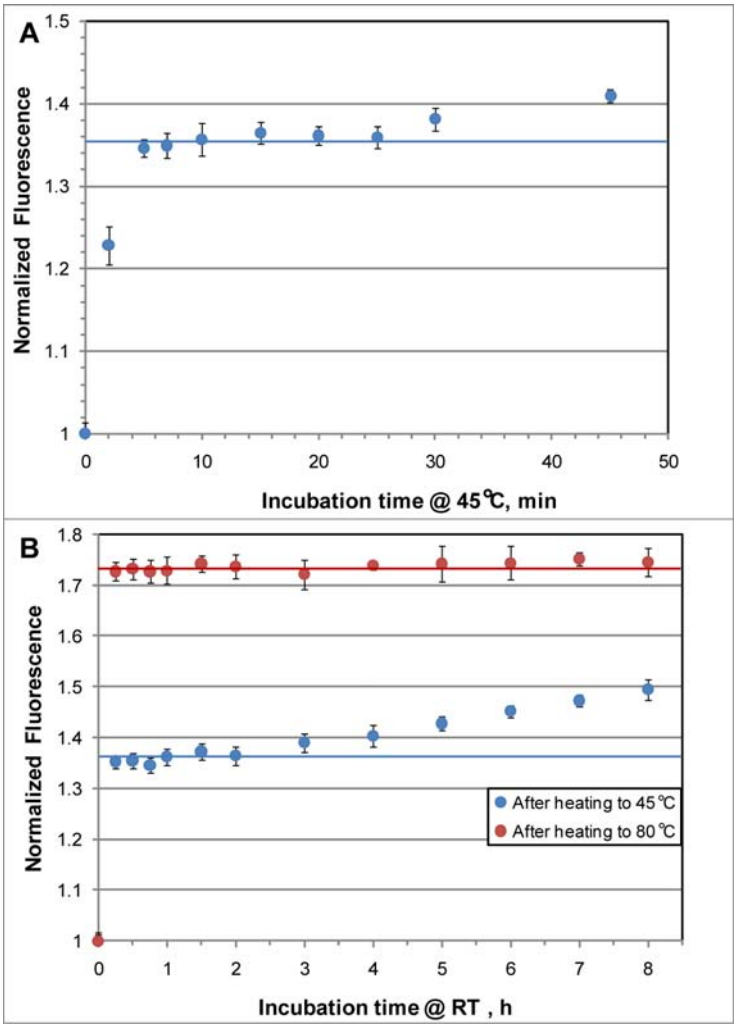

Figure S5. Dependence of the intrinsic fluorescence of β2AR-T4L/timolol in the MO cubic phase on the incubation times used in the LCP-Tm protocol.

(A) Several samples were heated to 45°C and incubated for different times (2-45 min). After incubation they were cooled down, centrifuged at 5,600 x *g* and 20°C for 10 min and assayed at RT. The fluorescence signals for all samples were normalized by the original signals recorded at RT before incubation. The same increase in the fluorescence was obtained for the samples incubated between 5 and 25 min.

(B) Two sets of samples were heated to 45°C or 80°C correspondingly, then cooled down and centrifuged at 5,600 x *g* and 20°C for 10 min. Intrinsic protein fluorescence was monitored at RT for up to 8 h after the temperature treatments.

All data points correspond to the averaged values obtained from at least three samples, and the error bars represent the standard deviations of these values.

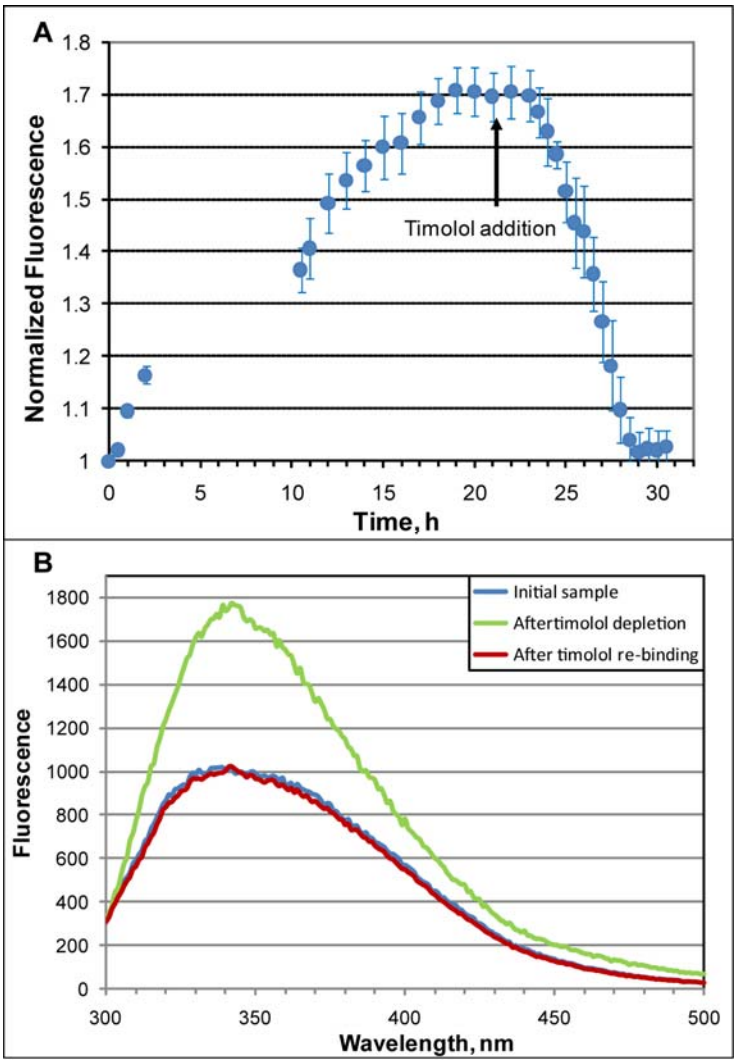

Figure S6. Ligand (timolol) release from and binding to β_2AR-T4L in the MO-based LCP. The ligand release kinetics was likely controlled by the ligand off-rate, while the ligand binding kinetics was limited by the ligand diffusion in LCP. For studies on diffusion of various size molecules from and to LCP see ref. 15. The intrinsic fluorescence data in (*A*) were normalized by the fluorescence of the initial sample. Data points in (*A*) correspond to the mean values, and the error bars represent the standard deviation errors of data recorded from 3 samples. During the ligand depletion section in (*A*) (0-22 h) the overlaid buffer was refreshed every hour except for the time period between 3 and 10 h. Corrected intrinsic fluorescence spectra for the initial sample bound to timolol (blue trace, time 0 h), after timolol depletion (green trace, time 21 h) and after timolol re-binding (red trace, 30 h) shown in (*B*) demonstrate the increase in fluorescence upon the ligand release and the reversibility of the signal upon the ligand re-binding.

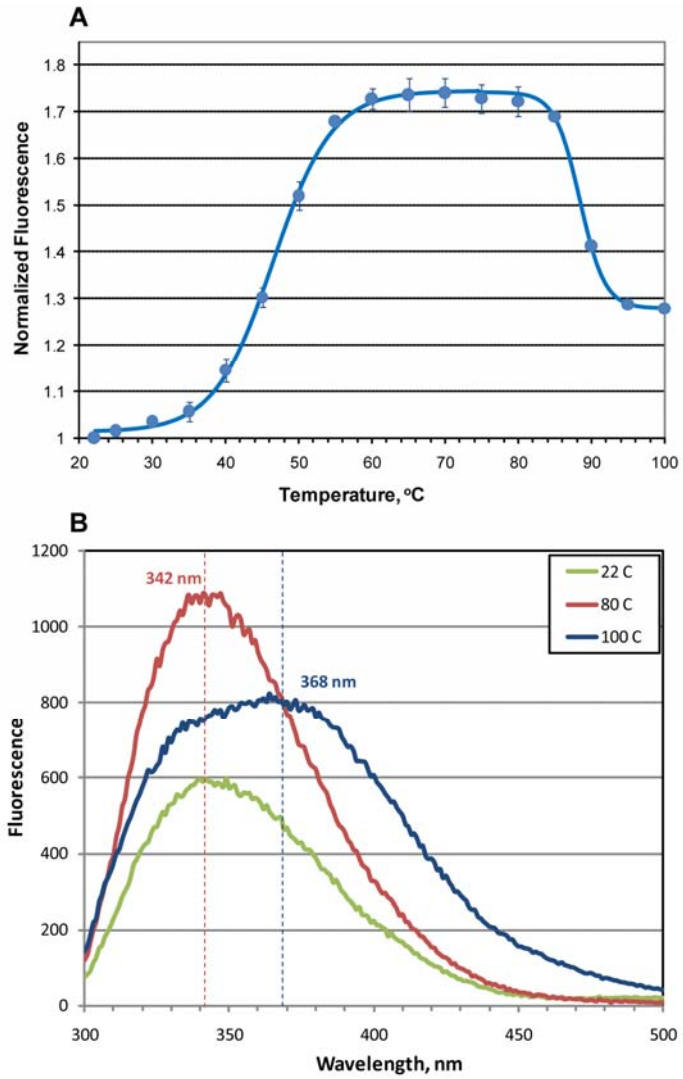

Figure S7. A thermal denaturation experiment with β_2AR-T4L/timolol in the MO-based LCP using the LCP-Tm protocol in the 22 – 100°C range.

(*A*) Changes in the intrinsic protein fluorescence recorded at RT after corresponding temperature treatments. (*B*) Intrinsic fluorescence spectra from the protein after representative temperature treatments.

The initial increase in the intrinsic protein fluorescence at ~47°C (*A*) corresponds to the temperature induced ligand release, accompanied by protein unfolding. The subsequent decrease in the intrinsic protein fluorescence at ~90°C (*A*) coincides with the cubic-Pn3m to hexagonal H_{II} phase transition in MO (see Fig. 2 *B*). The position of the intrinsic fluorescence maximum does not change and stays at ~342 nm during the first transition and shifts to ~368 nm during the second transition. The decrease and the red shift in the intrinsic protein fluorescence signal indicate that some tryptophan residues changed their environment into a more polar one upon disruption of the lipid bilayer during the cubic-Pn3m to H_{II} phase transition.

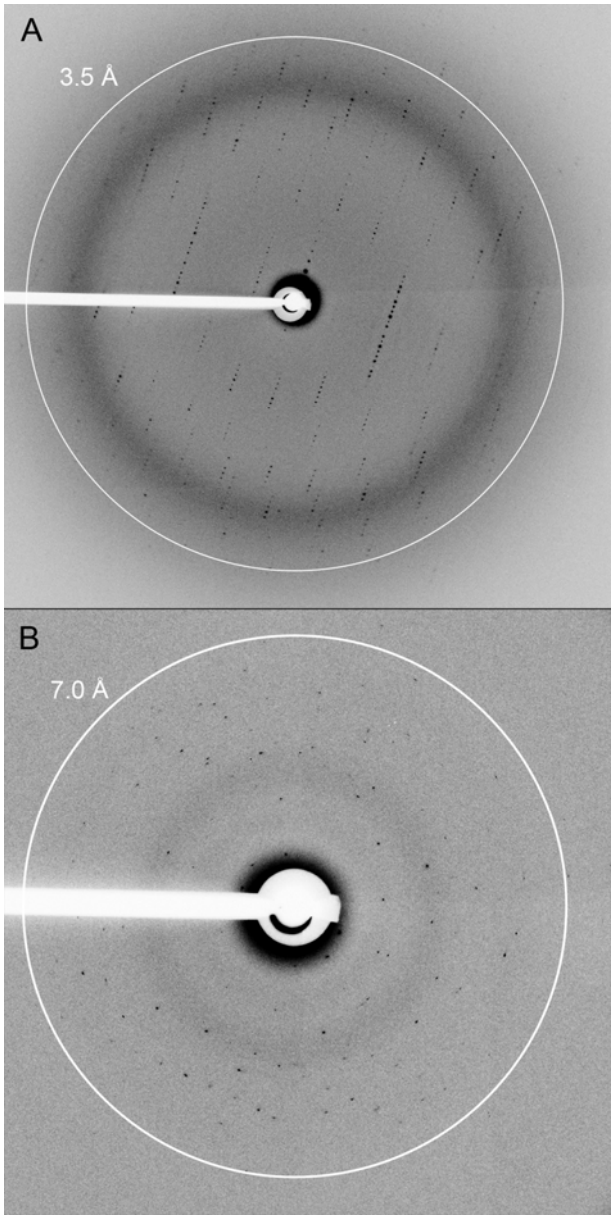

Figure S8. Diffraction images obtained from crystals of β_2AR-T4L bound to alprenolol (*A*) and clenbuterol (*B*). The data were collected on the beamline 23ID-B at GM/CA CAT at the Advance Photon Source (APS, Argonne National Lab, Argonne, IL) using a 10 micron mini-beam (12 keV), a MarMosaic 300 CCD detector (Rayonix, LLC, Evanston IL). The detector was positioned at a distance of 400 mm from the sample, and the sample was rotating 1 degree during the exposures of 1 s.

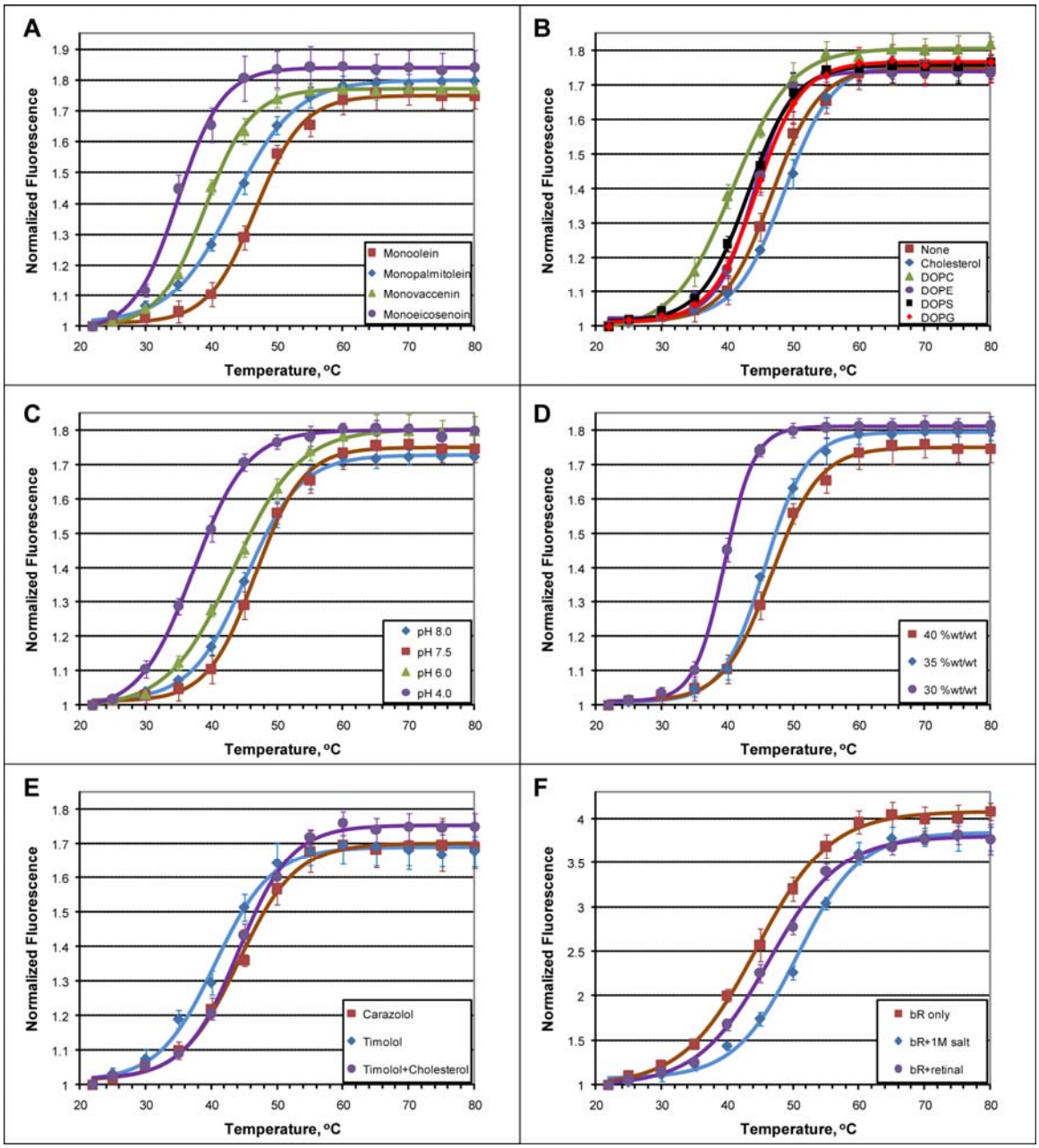

Figure S9. Thermal denaturation curves recorded by following the intrinsic protein fluorescence using the LCP-Tm protocol. (*A-D*) β_2AR-T4L, (*E*) β_2AR, (*F*) bR. β_2AR-T4L was bound to timolol in (*A-D)*. Solid lines represent fits by the Boltzmann sigmoidal function. Results of the curve fittings are shown in Table S3.
All data points correspond to the averaged values obtained from at least three samples, and the error bars represent the standard deviations of these values.

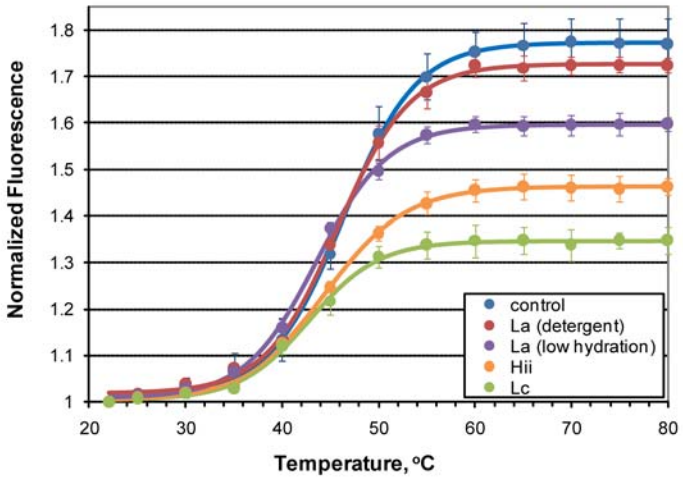

Figure S10. Effects of a transient passage through various mesophases on the thermal stability of β_2AR-T4L/timolol in the MO cubic phase. The decrease in the total change of the fluorescence signal indicates that a fraction of the protein was damaged upon transiently passing through the corresponding mesophase.
All data points correspond to the averaged values obtained from at least three samples, and the error bars represent the standard deviations of these values. The solid lines are fits by the Boltzmann sigmoidal function. Results of the curve fitting are shown in Table S3.

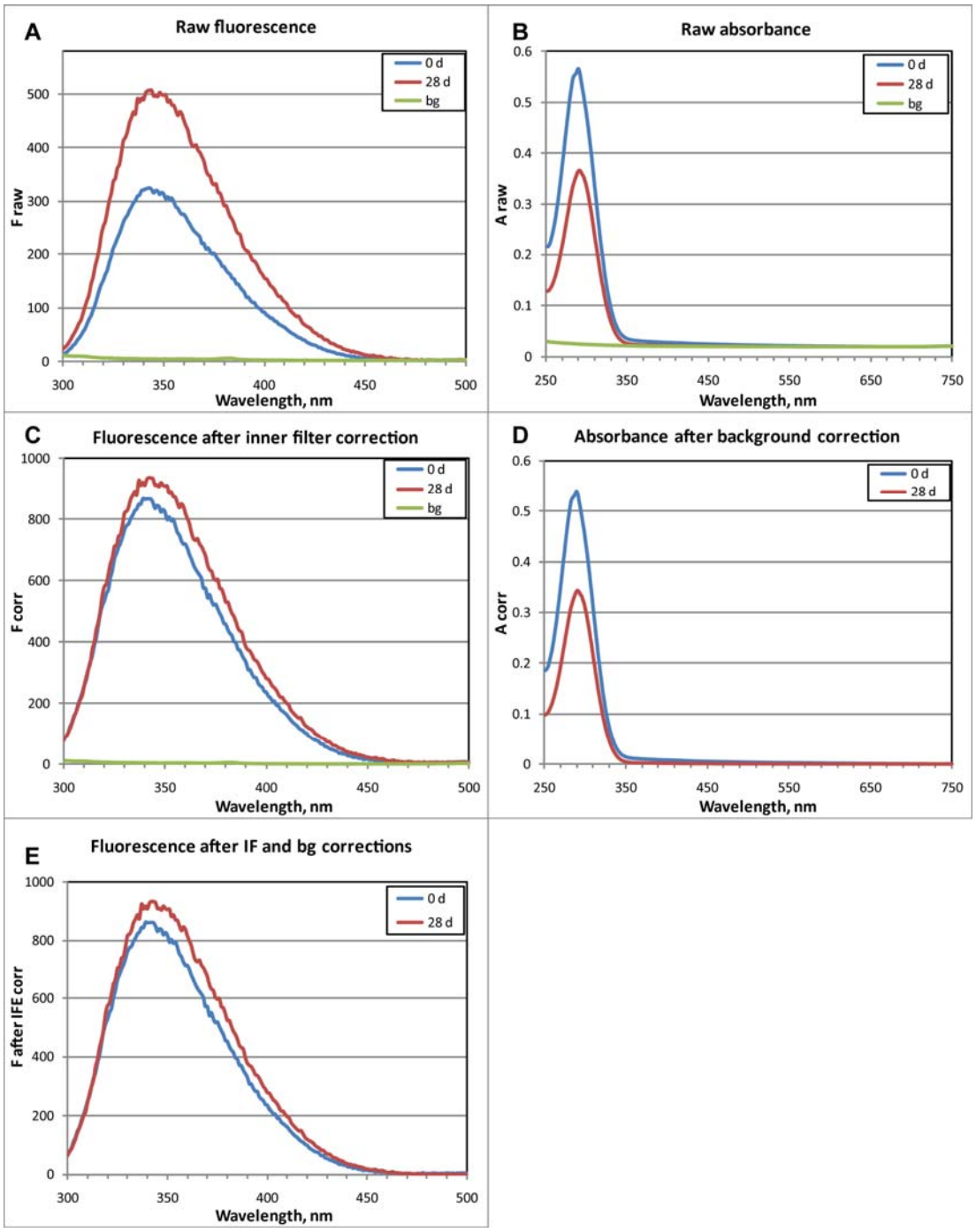

Figure S11. Raw and corrected intrinsic fluorescence and absorbance spectra for β_2AR-T4L/timolol in DDM/CHS solution collected at RT during the isothermal stability experiment. Only initial (0 d) and final (28 d) spectra are shown. Spectra of the background sample did not change with time.

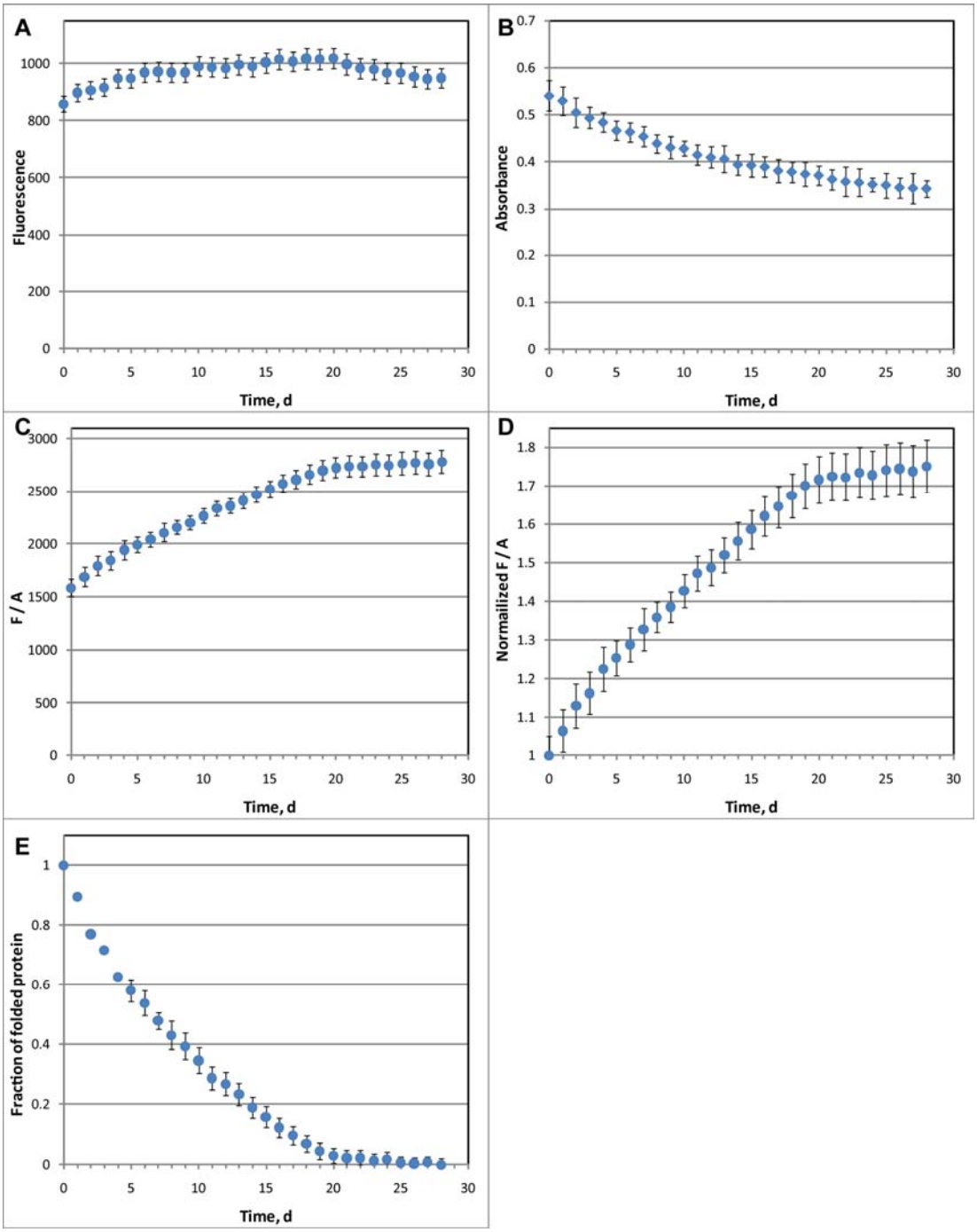

Figure S12. Changes in spectroscopic properties of β_2AR-T4L/timolol in DDM/CHS solution at RT with time.
(*A*) Maximum values of the corrected intrinsic fluorescence (see Fig. S11 *E*). (*B*) Maximum values of the corrected absorbance (see Fig. S11 *D*). Absorbance is proportional to the concentration of protein in solution. Decrease in the absorbance indicates protein precipitation which was removed from solution by centrifugation. (*C*) Fluorescence of the protein remaining in solution normalized to the absorbance of 1. (*D*) Normalized fluorescence of the protein remaining in solution (values in (*C*) normalized by the value at 0 d). The fluorescence increases due to the release of the ligand similarly to the thermal denaturation (Fig. S9) and the ligand release experiments (Fig. S6), reaching a saturated value of ~1.75, corresponding to a fully denatured protein. (*E*) Fraction of the folded protein remaining in solution in respect to the total protein was calculated from (*D*) and (*B*) assuming that all the protein was initially folded and that the normalized intrinsic fluorescence of a fully unfolded protein is 1.75.
All data points correspond to the averaged values obtained from three samples, and the error bars represent the standard deviations of these values.

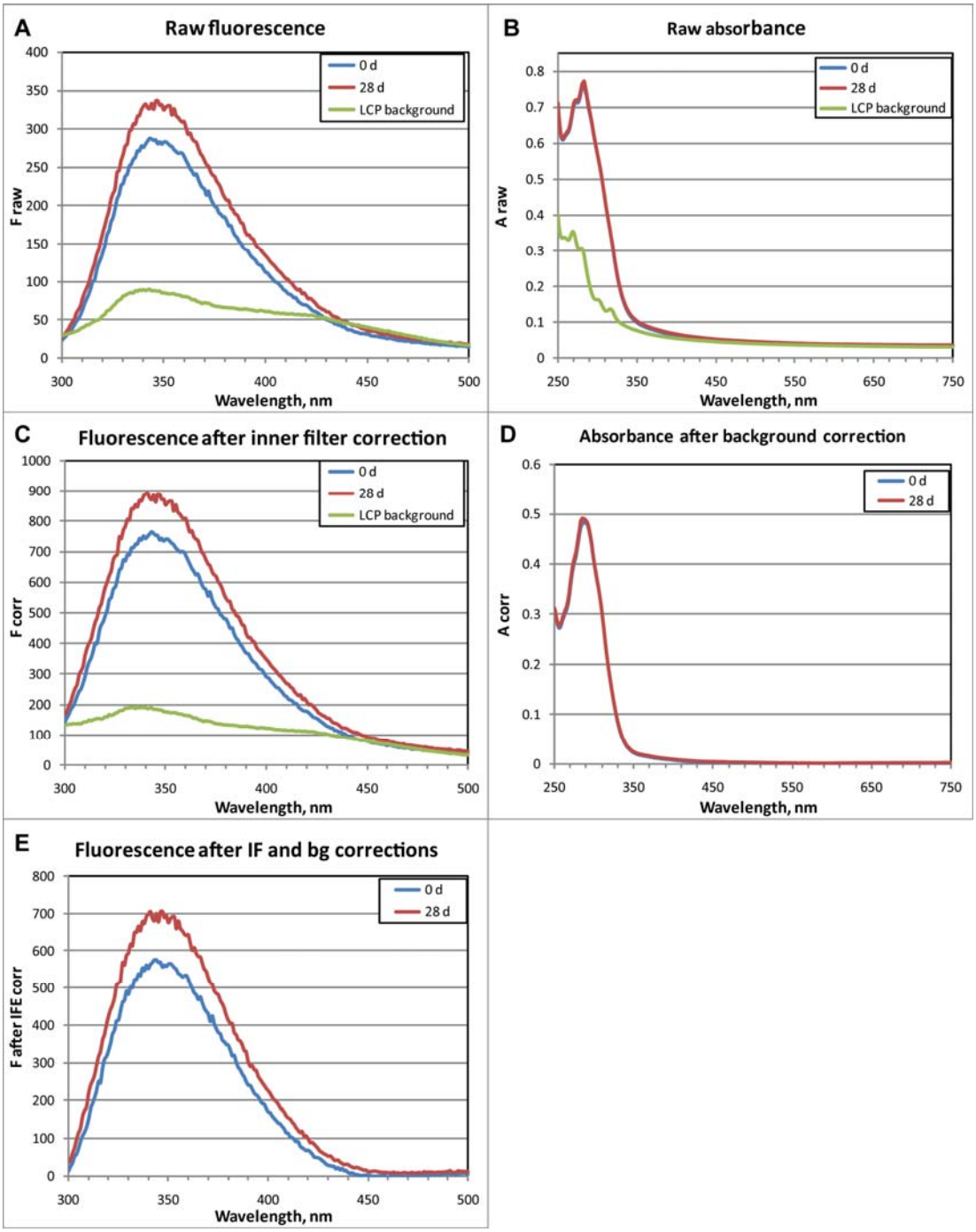

Figure S13. Raw and corrected fluorescence and absorbance spectra for β_2AR-T4L/timolol in the MO-based LCP collected at RT during the isothermal stability experiment. Only initial (0 d) and final (28 d) spectra are shown. Spectra of the background LCP sample did not change with time.

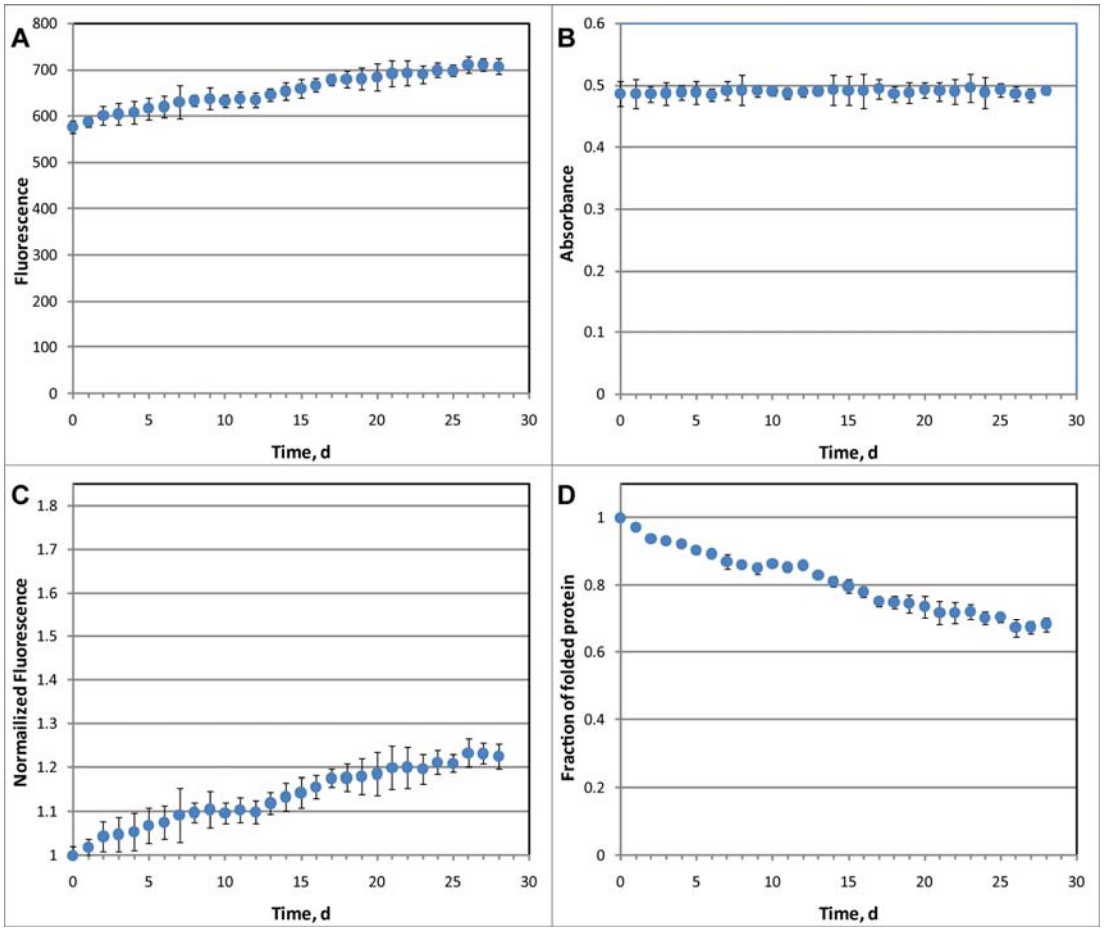

Figure S14. Changes in spectroscopic properties of β_2AR-T4L/timolol in the MO cubic phase at RT with time.

(*A*) Maximum values of the corrected intrinsic fluorescence (see Fig. S13 *E*).

(*B*) Maximum values of the corrected absorbance (see Fig. S13 *D*). Absorbance is proportional to the concentration of protein. A constant value of the absorbance indicates that concentration of the protein does not change.

(*C*) Normalized intrinsic protein fluorescence (values in (A) normalized by the value at 0 d). The fluorescence increases due to the release of the ligand similarly to the thermal denaturation (Fig. S9 and the ligand release experiments (Fig. S6).

(*D*) Fraction of the folded protein in LCP was calculated using the normalized intrinsic fluorescence signal (*C*) assuming that all the protein was initially folded and that the normalized intrinsic fluorescence of a fully unfolded protein equals 1.75 (see Fig. S12).

All data points correspond to the averaged values obtained from three samples, and the error bars represent the standard deviations of these values.

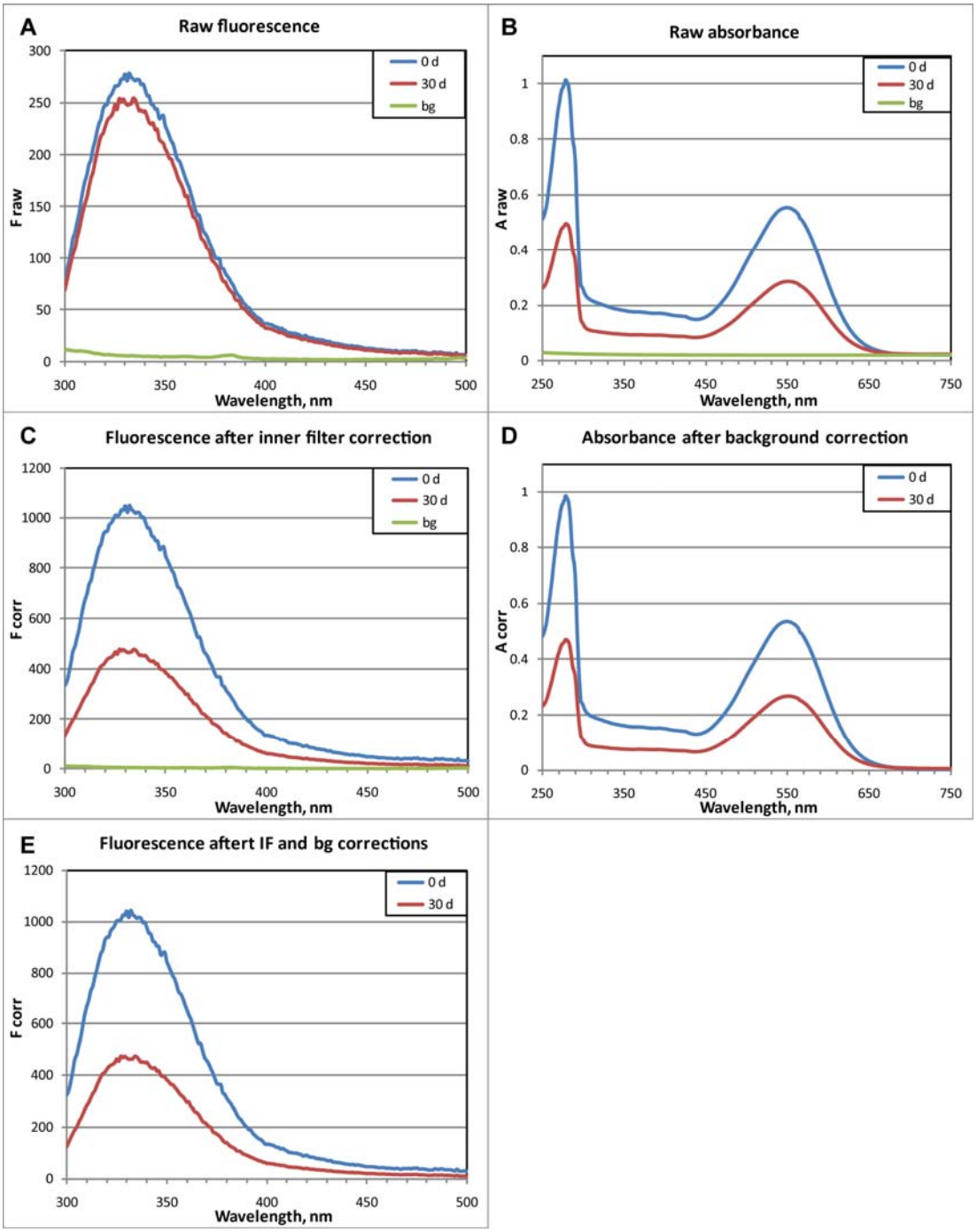

Figure S15. Raw and corrected fluorescence and absorbance spectra for bR in OG solution collected at RT during the isothermal stability experiment. Only initial (0 d) and final (30 d) spectra are shown. Spectra of the background sample did not change with time.

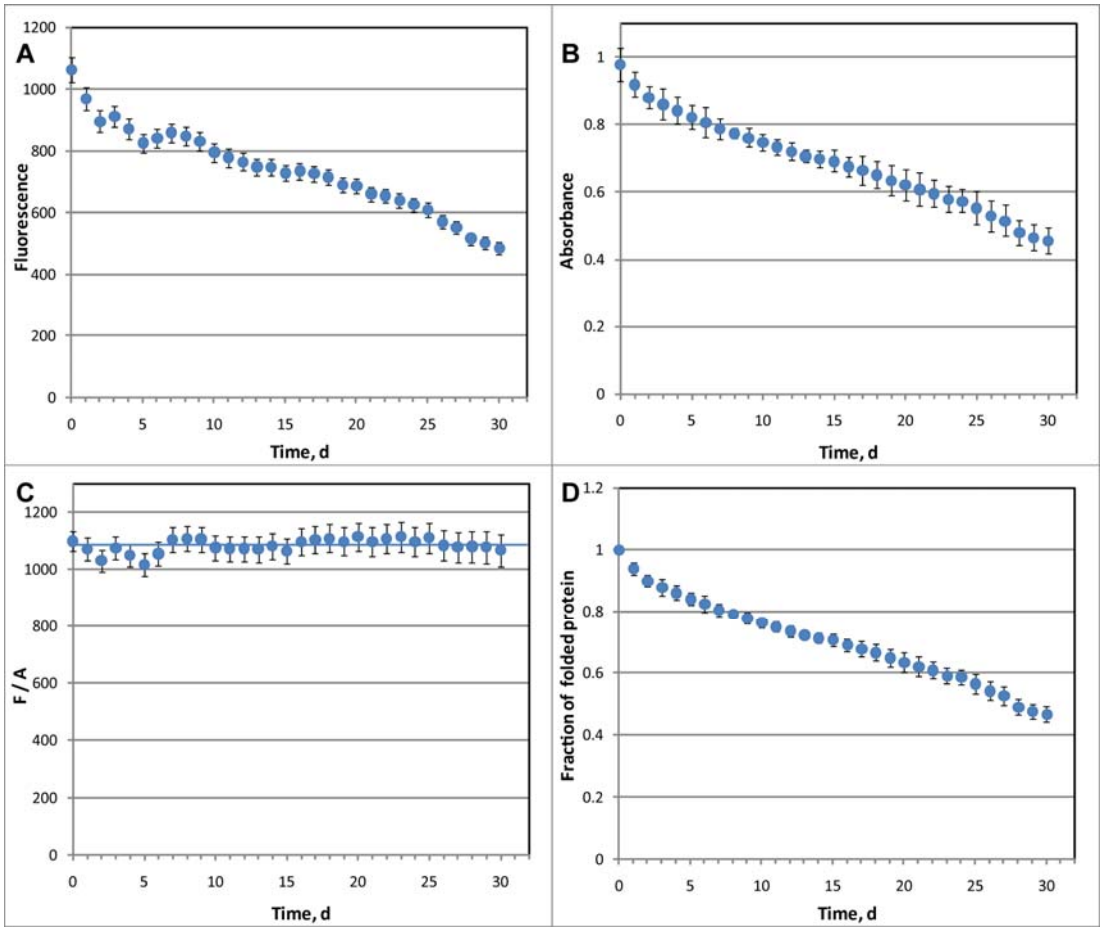

Figure S16. Changes in spectroscopic properties of bR in OG solution at RT with time.

(*A*) Maximum values of the corrected intrinsic fluorescence (see Fig. S15 *E*).

(*B*) Maximum values of the corrected absorbance (see Fig. S15 *D*). Absorbance is proportional to the concentration of protein in solution. Decrease in the absorbance indicates protein precipitation which was removed from solution by centrifugation.

(*C*) Fluorescence of the protein remaining in solution normalized to the absorbance of 1.The fluorescence does not change with time indicating that all the protein remaining in solution is folded. Denatured protein is presumably aggregated and removed from solution by centrifugation.

(*D*) Fraction of the folded protein remaining in solution in respect to the total protein was simply obtained by normalizing absorbance (*B*), since it had been established that all the protein in solution was folded.

All data points correspond to the averaged values obtained from three samples, and the error bars represent the standard deviations of these values.

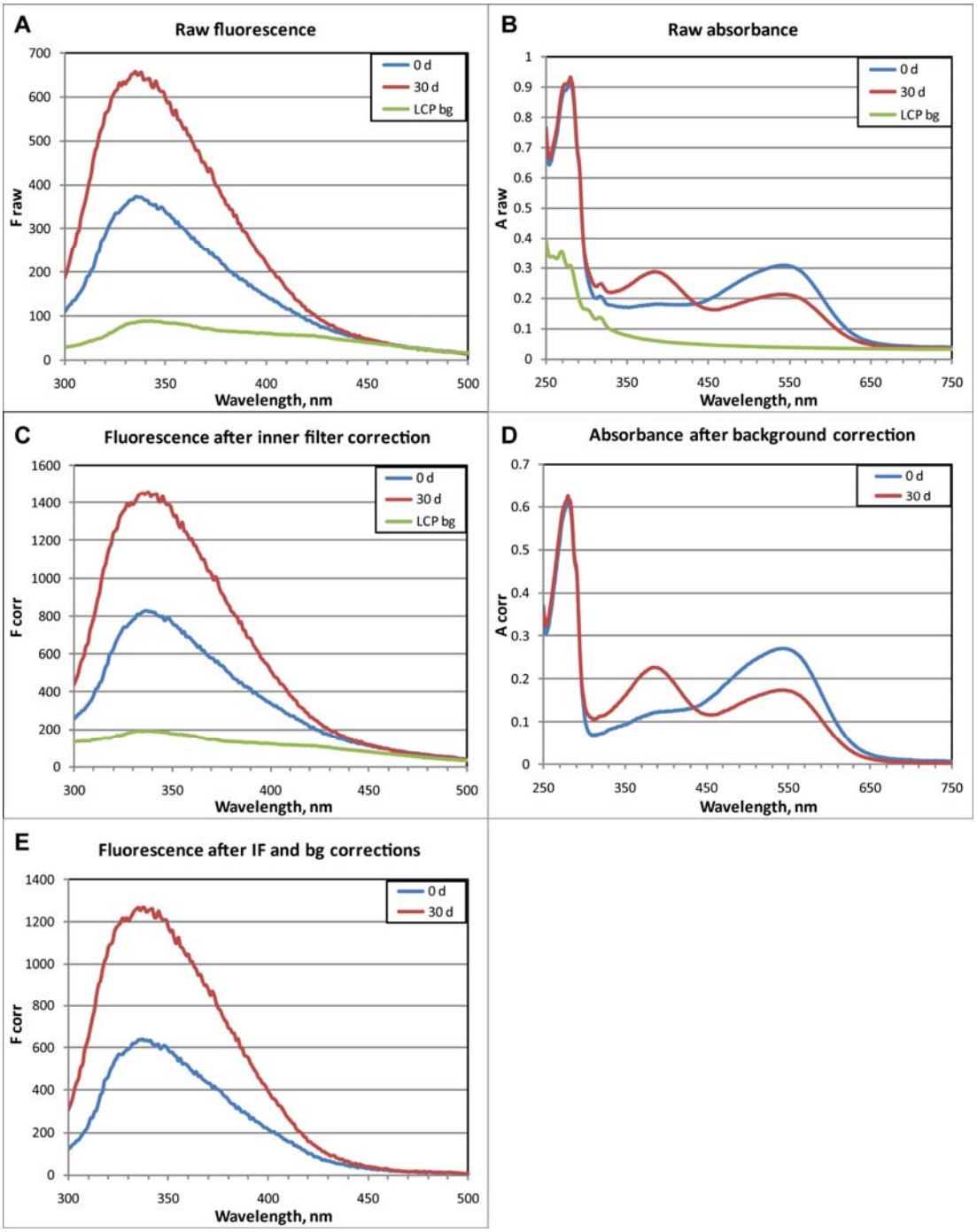

Figure S17. Raw and corrected fluorescence and absorbance spectra for bR in the MO-based LCP collected at RT during the isothermal stability experiment. Only initial (0 d) and final (30 d) spectra are shown. Spectra of the background LCP sample did not change with time. Absorption maximum of retinal strongly depends on the environment. In purple membranes the maximum absorbance of retinal bound to bR is at ~560 nm. When bR is solubilized in OG the absorbance maximum is at ~550 nm (Fig. S15 *D*). After insertion in the MO-based LCP the retinal absorbance maximum shifts to ~542 nm. Denaturation of bR is accompanied by a release of retinal. Free retinal absorbs at ~380 nm (*D*).

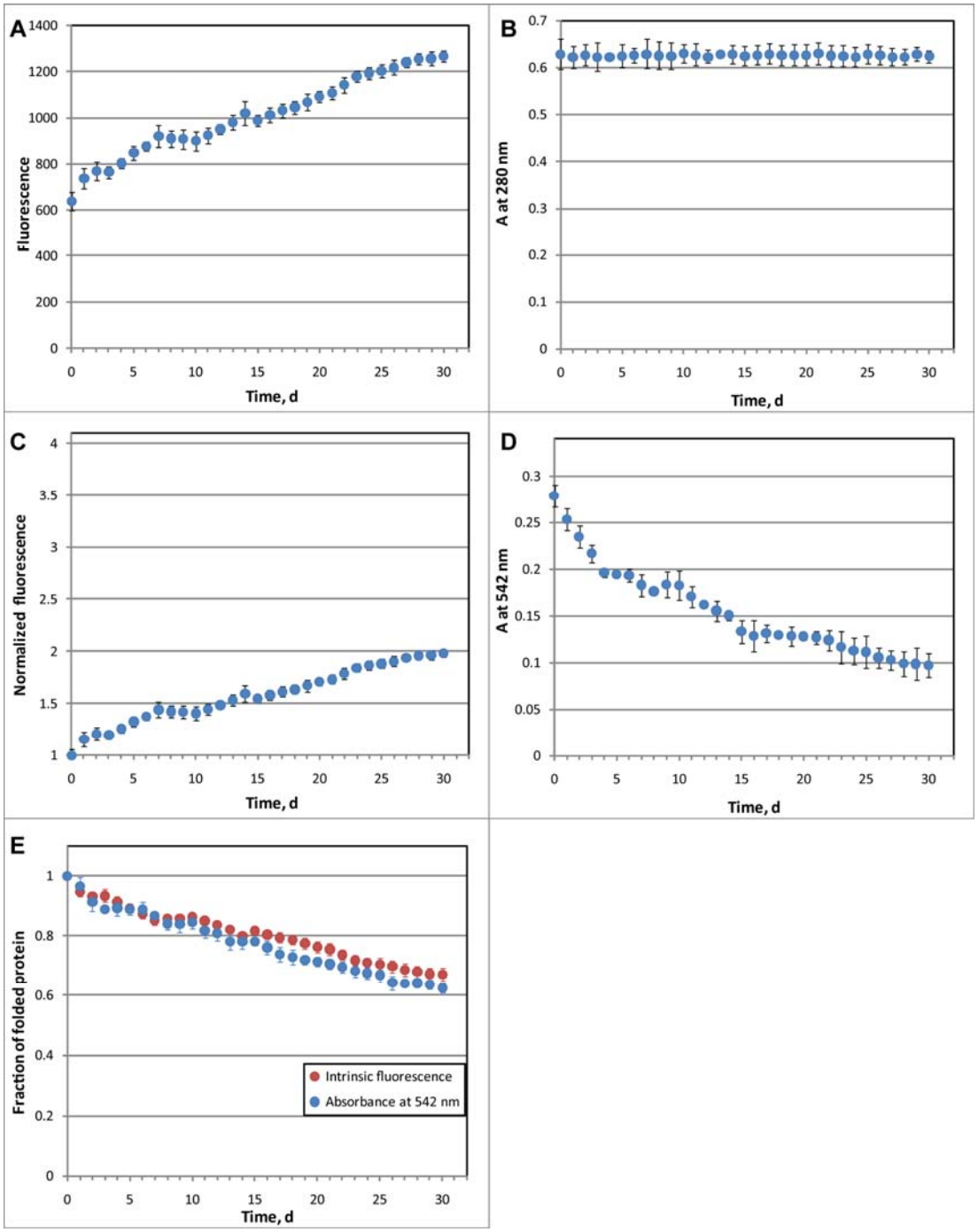

Figure S18. Changes in spectroscopic properties of bR in the MO cubic phase at RT with time.

(*A*) Maximum values of the corrected intrinsic fluorescence (see Fig. S17 *E*). (*B*) Corrected absorbance at 280 nm (see Fig. S17 *D*). The absorbance at 280 nm is proportional to the concentration of protein. A constant value of the absorbance indicates that concentration of the protein does not change. (*C*) Normalized intrinsic protein fluorescence (values in (A) normalized by the value at 0 d). The fluorescence increases due to the release of the ligand (retinal) similarly to the thermal denaturation (Fig. S9). (*D*) Corrected absorbance at 542 nm (see Fig. S17 *D*). The absorbance peak at 542 nm is proportional to the concentration of correctly folded protein. (*E*) Fraction of the folded protein in LCP estimated from the absorbance at 542 nm (blue circles) and using the intrinsic protein fluorescence (*C*) assuming that all the protein was initially folded and that the normalized intrinsic fluorescence of a fully unfolded protein equals 4 (see Fig. S9 *F*).

All data points correspond to the averaged values obtained from three samples, and the error bars represent the standard deviations of these values.

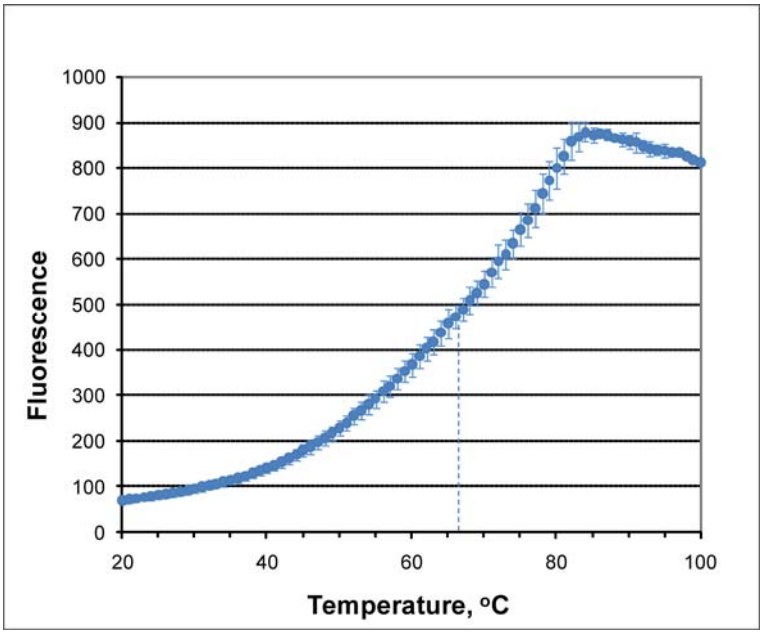

Figure S19. Thermal unfolding of β_2AR-T4L/timolol in 0.05 %w/v DDM, 0.01 %w/v CHS, 20 mM Hepes pH 7.5, 150 mM NaCl solution measured by a CPM assay (16). Data were acquired using excitation at 380 nm, emission at 462 nm and a temperature ramp of 1 °C/min. The apparent unfolding temperature is 66.1±1.2°C. Data points correspond to the averaged values from 3 samples. The error bars represent the standard deviation of these values.